IEEE Access
Multidisciplinary ⋮ Rapid Review ⋮ Open Access Journal

Received June 23, 2020, accepted July 21, 2020, date of publication August 3, 2020, date of current version August 12, 2020.

Digital Object Identifier 10.1109/ACCESS.2020.3013616

Cost-Efficient Bi-Layer Modeling of Antenna Input Characteristics Using Gradient Kriging Surrogates

ANNA PIETRENKO-DABROWSKA[1], (Senior Member, IEEE), SLAWOMIR KOZIEL[1,2], (Senior Member, IEEE), AND MU'ATH AL-HASAN[3], (Senior Member, IEEE)

[1]Faculty of Electronics, Telecommunications and Informatics, Gdansk University of Technology, 80-233 Gdansk, Poland
[2]Engineering Optimization and Modeling Center, Department of Technology, Reykjavik University, 101 Reykjavik, Iceland
[3]Networks and Communication Engineering Department, Al Ain University, Abu Dhabi, United Arab Emirates

Corresponding author: Anna Pietrenko-Dabrowska (anna.dabrowska@pg.edu.pl)

This work was supported in part by the Icelandic Centre for Research (RANNIS) under Grant 206606051, in part by the National Science Centre of Poland under Grant 2017/27/B/ST7/00563, and in part by the Abu-Dhabi Department of Education and Knowledge (ADEK) Award for Research Excellence, in 2019, under Grant AARE19-245.

ABSTRACT Over the recent years, surrogate modeling has been playing an increasing role in the design of antenna structures. The main incentive is to mitigate the issues related to high cost of electromagnetic (EM)-based procedures. Among the various techniques, approximation surrogates are the most popular ones due to their flexibility and easy access. Notwithstanding, data-driven modeling of antenna characteristics is associated with serious practical issues, the primary one being the curse of dimensionality, particularly troublesome due to typically high nonlinearity of antenna responses. This limits applicability of conventional surrogates to simple structures described by a few parameters within narrow ranges thereof, which is grossly insufficient from the point of view of design utility. Many of these issues can be alleviated by the recently proposed constrained modeling techniques that restrict the surrogate domain to regions containing high-quality designs with respect to the relevant performance figures, which are identified using the pre-optimized reference designs at an extra computational effort. This paper proposes a methodology based on gradient-enhanced kriging (GEK). It enables a considerable reduction of the number of reference points required to construct the inverse surrogate (employed in surrogate model definition) by incorporating the sensitivity data into the nested kriging framework. Using two antenna examples, it is demonstrated to yield significant savings in terms of the surrogate model setup cost as compared to both conventional modeling methods and the original nested kriging.

INDEX TERMS Antenna modeling, surrogate modeling, two-stage modeling, gradient kriging, domain confinement, simulation-driven design, design optimization.

I. INTRODUCTION

Full-wave electromagnetic (EM) simulation tools have become ubiquitous in the design of contemporary antenna systems [1]–[3]. This is partially related to continuously increasing geometrical complexity of antenna structures but also the necessity of including immediate environment of the radiators (e.g., connectors [4], housing [5]), and accounting for the phenomena that have non-negligible effects on operation (e.g. mutual coupling within antenna arrays [6] or MIMO systems [7], etc.). The former is a consequence of growing demands on antenna performance dictated by modern applications (e.g., 5G technology [8], medical imaging [9], internet of things (IoT) [10]) and functionality requirements (e.g., multi-band operation [11], circular polarization [12], pattern diversity [13]). In many cases, a reduction of the antenna footprint is also of concern, e.g., for wearable [14] and implantable devices [15]. This leads to further challenges as miniaturization generally stays in conflict with maintaining acceptable electrical and field characteristics. In either case, EM analysis is not only required for design verification but even more to carry out the design process itself. A widely applied procedure is the final parameter tuning (or design closure) [16]. Depending on the circumstances, it may entail local [17] or global search [18], both associated with considerable computational costs. This prompts

The associate editor coordinating the review of this manuscript and approving it for publication was Yue Zhang.

many researchers and practitioners to default to interactive design routines, largely rooted in experience-driven parameter sweeping. Needless to say, such methods are incapable of identifying truly optimum parameter sets, let alone to efficiently handle multiple objectives and constraints inherent to modern antenna design [19].

Accelerating EM-driven design procedures has been the subject of extensive research [20]–[35]. In the context of design optimization, several classes of methods have been developed. For example, the cost of gradient-based algorithms can be reduced by employing adjoint sensitivities [20], or through the development of sparse sensitivity updating schemes [21], [22]. Another option is utilization of variable-fidelity simulations, where the low-fidelity models (e.g., equivalent networks [23], or coarse-mesh EM simulations [24]) can be used—upon suitable enhancement—as reliable predictors replacing high-fidelity EM analysis in seeking for the best possible design. Some of the representative methods of this group include space mapping [25], manifold mapping [26], adaptive response scaling [27], feature-based optimization [28], or cognition-driven design [29]. Approximation-based metamodels are also popular in this context (e.g., polynomial regression [30], kriging [31], neural networks [32]), along with machine learning methods, which are especially suitable for global optimization [33], [34].

The aforementioned methodologies generally attempt to expedite the design procedures by purely algorithmic means or incorporating (sparsely executed) EM analyses into construction-prediction loops that involve data-driven or physics-based metamodels. In principle, a more appealing approach would be to replace expensive computational models by fast surrogates altogether. A clear advantage is a possibility to carry out all kinds of simulation-driven tasks, including design closure, at essentially negligible costs. From this perspective, approximation surrogates are particularly attractive as being only dependent on the sampled simulation data with no need to engage any problem-specific knowledge. Another reason is the availability of numerous and well-established techniques, among others, polynomial regression [35], radial-basis functions (RBF) [36], kriging [35], neural networks [36], support vector regression (SVR) [37], Gaussian process regression [38], or polynomial chaos expansion [39]. The downside of conventional data-driven methods is a rapid increase of the training data set size necessary to render a reliable surrogate (as a function of the number of the system variables and the ranges thereof), known as the curse of dimensionality [40]. Because modern antenna structures are typically described by many parameters, and design-ready models have to cover broad ranges of operating conditions, the aforementioned issues constitute a serious limitation. High nonlinearity of antenna characteristics only adds to these challenges. Several attempts to mitigate the dimensionality problems resulted in the development of techniques such as high-dimensional model representation (HDMR) [41], least-angle regression [42], but also variable-fidelity methods that aim at blending sparsely-sampled high-fidelity data with densely sampled low-fidelity (thus less expensive) simulations, e.g., co-kriging [43], two-stage GPR [44], Bayesian model fusion [45].

Traditionally, surrogate models are established in interval-type of domains, delimited by the lower and upper bounds for the system parameters. Such domains are easy to handle, both in terms of design of experiments and subsequent model optimization. However, given any set of performance figures that is relevant for the design problem at hand, ''good'' designs (i.e., being of high-quality with respect to these performance figures) occupy a small region of the box-constrained space. The latter is determined by the correlations between the optimum sets of parameters. For example, dimension scaling of an antenna w.r.t. the operating frequency requires synchronized adjustment of at least of some of its geometry parameters. The recently reported constrained (or performance-driven) modeling concept [46]–[48] employs this observation to restrict the surrogate model domain to such promising regions. The advantages are twofold: significant savings in terms of the number of training data samples, and a possibility of constructing reliable surrogates over wide ranges of antenna parameters and its operating conditions. The recent technique adopting this approach is the nested kriging, where two kriging interpolation models are generated: the first-level one to define the domain, and the second-level model being the actual surrogate [48].

Within the performance-driven modeling paradigm, the surrogate model domain is determined using the sets of pre-existing designs, optimized for the selected sets of performance specifications. These reference points are allocated uniformly within the objective space to provide reliable information concerning distribution of the optimum designs in the parameter space of the antenna at hand. Construction of a high-accuracy model within the constrained domain requires a small number of training samples (typically, a few hundred), even if the parameter space dimensionality is relatively high ($n > 10$) [48]. Compared to the low cost of training data acquisition, the initial effort related to obtaining the reference designs (typically up to 10-12 two-dimensional objective space and 16-20 for three-dimensional space [47]) may be relatively high or may even become the major contributor to the overall cost of setting up the surrogate.

This paper proposes an alternative approach to defining the surrogate model domain for performance-driven frameworks. Our methodology is based on gradient enhanced kriging (GEK) [49] and permits a significant reduction of the number of reference designs without compromising the model reliability. For the sake of demonstration, it is incorporated into nested kriging and demonstrated using two antenna examples. The reduction of the number of reference designs is significant: from twenty seven to only eight for the first antenna, and from eight to four for the second structure. The predictive power of the surrogate models obtained with the original and GEK-based approaches is comparable, and by far exceeding the accuracy of conventional models.

II. TWO-STAGE PERFORMANCE-DRIVEN MODELING USING GRADIENT ENHANCED KRIGING

This section outlines the proposed approach to surrogate model definition using gradient-enhanced kriging (GEK) [49] along with incorporation of the concept into the nested kriging modelling framework. The subsequent sub-sections explain the overall concept of performance-driven modelling, briefly recall the formulation of GEK, as well as provide the details on GEK-based first-level model of the nested kriging. The primary objective is a reduction of the number of reference designs required for domain confinement without compromising the reliability of the modelling process.

A. PERFORMANCE-DRIVEN MODELING CONCEPT

Performance-driven modeling [47] focuses construction of the surrogate in the region containing designs optimal with respect to a given set of performance figures (e.g., allocating the multi-band antenna resonances at required operating frequencies [48]). The volume of such a region is significantly smaller than the volume of a conventional box-constrained domain X determined by the lower/upper bounds for design parameters $\boldsymbol{l} = [l_1 \ldots, l_n]^T$ and $\boldsymbol{u} = [u_1 \ldots, u_n]^T$. This enables computational savings in terms of training data acquisition.

Let $\boldsymbol{x} = [x_1 \ldots x_n]^T$ be the vector of antenna parameters. We also denote by f_k, $k = 1, \ldots, N$, the figures of interest relevant to the design task at hand. These may include the operating conditions (operating frequency, bandwidth) but also material parameters (e.g., substrate permittivity). The objective space F, defined by the ranges $f_{k.\min} \leq f_k^{(j)} \leq f_{k.\max}$, $j = 1, \ldots, p$, $k = 1, \ldots, N$, determines the intended region of validity of the surrogate model.

The central concept of performance-driven modeling is the optimum design set $X^*(F)$ which is generally an N-dimensional manifold in the parameter space X, defined as

$$X^*(F) = \{U_F(\boldsymbol{f}) : \boldsymbol{f} \in F\} \tag{1}$$

where $X^*(\boldsymbol{f})$ is the optimum design for the objective vector $\boldsymbol{f} = [f_1 \ldots f_N]^T \in F$. Assuming a scalar merit function $U(\boldsymbol{x}, \boldsymbol{f})$ quantifying the utility of the design $\boldsymbol{x}$ with respect to the target objective vector $\boldsymbol{f}$, $X^*(\boldsymbol{f})$ is obtained by solving

$$\boldsymbol{x}^* = X^*(\boldsymbol{f}) = \arg\min_{\boldsymbol{x}} U(\boldsymbol{x}, \boldsymbol{f}) \tag{2}$$

Note that rendering the surrogate modeling within $X^*(F)$ is sufficient to capture all designs that are optimum over a given objective space F. In practice, $X^*(F)$ can only be approximated using limited available data. In performance-driven modeling, this information is assumed in the form of the reference designs $\boldsymbol{x}^{(j)} = [x_1^{(j)} \ldots x_n^{(j)}]^T$, $j = 1, \ldots, p$, optimized w.r.t. the selected objective vectors $\boldsymbol{f}^{(j)} = [f_1^{(j)} \ldots f_N^{(j)}]$ [48]. It is advantageous to allocate $\boldsymbol{f}^{(j)}$ uniformly within F. In some cases, $\boldsymbol{x}^{(j)}$ may be available from the previous design work with the same antenna structure. In general, the reference designs have to be obtained specifically for the purpose of surrogate model construction. This entails considerable computational expenditures because p independent optimization runs are required to yield the set $\{\boldsymbol{x}^{(j)}\}_{j=1,\ldots,p}$.

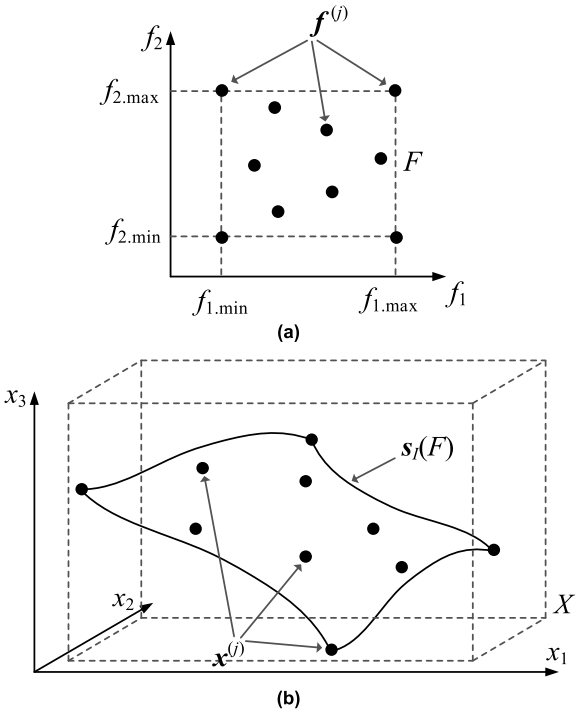

FIGURE 1. Basic components of performance-driven modeling using nested kriging, illustrated for two performance figures and three-dimensional parameter space: (a) objective space F and reference objective vectors $f^{(j)}$ (b) parameter space X, the reference designs $x^{(j)}$, and the first-level model image $s_l(F)$.

A particular way of employing the reference points to approximate the optimum set $X^*(F)$ is method-specific [46]–[48]. Here, we focus on the nested kriging framework [48], where the geometry of $X^*(F)$ is estimated using the first-level surrogate $\boldsymbol{s}_l(\boldsymbol{f})$: $F \rightarrow X$, identified as a kriging interpolation model with $\{\boldsymbol{f}^{(j)}, \boldsymbol{x}^{(j)}\}$, $j = 1, \ldots, p$, being the training set (cf. Fig. 1).

It should be reiterated that the purpose of the first-level model is to approximate the optimum design set $X^*(F)$, which is where the surrogate model is to be established. Restricting the modelling process to $X^*(F)$ and its vicinity is the major factor that allows us to improve the computational efficiency of the modelling process by a dramatic reduction of the surrogate model domain and by rendering the surrogate only in the areas that contain high-quality antenna designs (w.r.t. the assumed performance figures).

B. GRADIENT ENHANCED KRIGING

Kriging is a popular data-driven technique for interpolating deterministic noise-free data [35]. Gradient-enhanced kriging (GEK) [49] is a variation of kriging, which incorporates—apart from the system outputs—also their gradients at the observation points. GEK is utilized in this work to reduce the number of reference designs that is required to approximate

the optimum design set $X^*(F)$. This section gives a brief outline of the gradient kriging. A more in-depth treatment of the subject can be found in the extensive literature, e.g., [35], [49], [50].

We start by explaining ordinary kriging (OK), where the output $f(\boldsymbol{x})$ of the system of interest is assumed to be of the form

$$y(\boldsymbol{x}) = \mu + Z(\boldsymbol{x}) \tag{3}$$

where $\boldsymbol{x}$ is the vector of designable parameters (cf. Section 2.1), μ is the constant trend function (which, in principle, may take the more generic form of $\boldsymbol{g}(\boldsymbol{x})^T\boldsymbol{\beta}$, e.g., a low-order polynomial [43]), and $Z(\boldsymbol{x})$ is a realization of a normally distributed Gaussian random process with zero mean and variance σ^2. $Z(\boldsymbol{x})$ takes into account localized variations from the mean μ.

The correlations between $Z(\boldsymbol{x}^{(i)})$ and $Z(\boldsymbol{x}^{(j)})$ at the two observation points $\boldsymbol{x}^{(i)}$ and $\boldsymbol{x}^{(j)}$, $i, j = 1, \ldots, p$, are described by the correlation function, e.g., Gaussian [35]

$$R_{ij} = corr\left[Z(\boldsymbol{x}^{(i)}), Z(\boldsymbol{x}^{(j)})\right] = \\ = \exp\left(-\sum\nolimits_{k=1}^{n} \theta_k |x_k^{(i)} - x_k^{(j)}|^2\right) \tag{4}$$

or Matern 3/2 [49]

$$R_{ij} = \left(1 + \sqrt{3\sum\nolimits_{k=1}^{n} \theta_k |x_k^{(i)} - x_k^{(j)}|^2}\right) \cdot \\ \cdot \exp\left(-\sqrt{3\sum\nolimits_{k=1}^{n} \theta_k |x_k^{(i)} - x_k^{(j)}|^2}\right) \tag{5}$$

Ordinary kriging predicts the system output at the location $\boldsymbol{x}$ as

$$s(\boldsymbol{x}) = \mu + \boldsymbol{r}(\boldsymbol{x})^T \boldsymbol{\Psi}^{-1}(\boldsymbol{y} - \boldsymbol{1}\mu) \tag{6}$$

where $\boldsymbol{r}(\boldsymbol{x})$ is the vector of correlations between the p data points $\boldsymbol{x}^{(j)}$ and $\boldsymbol{x}$, whereas Ψ is a symmetric $p \times p$ matrix of correlations R_{ij} (cf. (4) and (5)); $\boldsymbol{1}$ is the vector of ones, whereas $\boldsymbol{y}$ is the vector of the system outputs at $\boldsymbol{x}^{(j)}$, $j = 1, \ldots, p$. Model identification requires optimizing the vector $\theta = [\theta_1 \ldots \theta_n]^T$ of hyperparameters, which is accomplished by maximum likelihood [35], i.e., maximizing $-[p\ln(\sigma^2) + \ln|\boldsymbol{\Psi}|]/2$ with both σ^2 and $\boldsymbol{\Psi}$ being functions of θ.

Gradient-enhanced kriging can be considered a multi-data extension to kriging [49]. The correlation matrix for GEK, denoted as $\dot{\boldsymbol{\Psi}}$, is defined as

$$\dot{\boldsymbol{\Psi}} = \begin{bmatrix} \boldsymbol{\Psi} & \dfrac{\partial \boldsymbol{\Psi}}{\partial \boldsymbol{x}^{(i)}} \\ \dfrac{\partial \boldsymbol{\Psi}}{\partial \boldsymbol{x}^{(j)}} & \dfrac{\partial^2 \boldsymbol{\Psi}}{\partial \boldsymbol{x}^{(i)} \partial \boldsymbol{x}^{(j)}} \end{bmatrix} \tag{7}$$

The GEK prediction is performed based on the set of observations $\boldsymbol{x}^{(j)}$, $j = 1, \ldots, p$, and the observed data $\boldsymbol{y} = [y(\boldsymbol{x}^{(1)}) \ldots y(\boldsymbol{x}^{(p)}) \; \partial y(\boldsymbol{x}^{(1)})/\partial x_1 \ldots \partial y(\boldsymbol{x}^{(p)})/\partial x_1 \ldots \partial y(\boldsymbol{x}^{(1)})/\partial x_n \ldots \partial y(\boldsymbol{x}^{(p)})/\partial x_n]^T$. We have

$$s_{GEK}(\boldsymbol{x}) = \mu + \dot{\boldsymbol{r}}(\boldsymbol{x})^T \dot{\boldsymbol{\Psi}}^{-1}(y - \boldsymbol{1}\mu) \tag{8}$$

in which the correlation vector $\dot{\boldsymbol{r}}(\boldsymbol{x}) = \left[\boldsymbol{r}^T (\partial \boldsymbol{r}/\partial x_1)^T \ldots (\partial \boldsymbol{r}/\partial x_n)^T\right]$. The mean of the kriging regression is obtained using the generalized least squares as $\mu = (\boldsymbol{1}^T \dot{\boldsymbol{\Psi}}^{-1} \boldsymbol{1})^{-1} \boldsymbol{1}^T \dot{\boldsymbol{\Psi}}^{-1} \boldsymbol{y}$. The hyperparameters θ are estimated similarly as for OK using maximum likelihood [49].

Both OK and GEK can be generalized to vector-valued outputs, in particular, the antenna responses $\boldsymbol{R}(\boldsymbol{x})$, in a straightforward manner.

C. NESTED-KRIGING FRAMEWORK WITH GEK-BASED FIRST-LEVEL MODEL

Our goal is to reduce the number of reference designs required to construct the first-level model $\boldsymbol{s_I}(\boldsymbol{f})$ of the nested kriging. As explained in Section 2.1, $\boldsymbol{s_I}(\boldsymbol{f})$ is effectively an inverse surrogate identified using the pairs $\{\boldsymbol{f}^{(j)}, \boldsymbol{x}^{(j)}\}$, $j = 1, \ldots, p$, where $\boldsymbol{f}^{(j)}$ are the objective vectors and $\boldsymbol{x}^{(j)}$ are the antenna parameter vectors optimized in the sense of (2). Because $\boldsymbol{s_I}(F)$ is a low-dimensional manifold in X (typically, the number of performance figures is a few, e.g., two or three), gradient-enhanced kriging (cf. Section 2.2) is a suitable tool to limit p by incorporating the sensitivity data $\boldsymbol{J}^x(\boldsymbol{f}) = \partial \boldsymbol{x}/\partial \boldsymbol{f} = \partial X^*(\boldsymbol{f})/\partial \boldsymbol{f}$. The entries J^x_{jk} of the Jacobian $\boldsymbol{J}^x(\boldsymbol{f})$ are the partial derivatives of the (optimized) antenna geometry parameters x_j with respect to the performance figures f_k. These derivatives are not directly available; however, they can be estimated using the antenna response sensitivities that are already known as a by-product of solving (2) (identification of the reference designs). We denote by $\boldsymbol{R}(\boldsymbol{x})$ the response of the EM simulation model of the antenna at hand and by $\boldsymbol{J}(\boldsymbol{x})$ its Jacobian matrix at the design $\boldsymbol{x}$.

Let $\boldsymbol{d} = [d_1 \ldots d_N]^T$ denote a vector of perturbations of the performance figures. At the first step, we find the perturbed reference designs $\boldsymbol{x}^{(j.k)}$ corresponding to vectors $[f_1^{(j)} \ldots f_k^{(j)} + d_k \ldots f_N^{(j)}]^T$

$$\boldsymbol{x}^{(j.k)} = \arg\min_{\boldsymbol{x}} U_L(\boldsymbol{x}; f_1^{(j)}, \ldots, f_k^{(j)} + d_k, f_N^{(j)}) \tag{9}$$

in which the objective function U_L is based on the first-order Taylor expansion of $\boldsymbol{R}$

$$\boldsymbol{R}(\boldsymbol{x}) = \boldsymbol{R}(\boldsymbol{x}^{(j)}) + \boldsymbol{J}(\boldsymbol{x}^{(j)}) \cdot (\boldsymbol{x} - \boldsymbol{x}^{(j)}) \tag{10}$$

This ensures that the cost of solving (9) is negligible (as mentioned above, $\boldsymbol{J}(\boldsymbol{x})$ are known beforehand). The actual values of the figures interest $[f_1^{(j.k)} \ldots f_N^{(j.k)}]^T$, corresponding to $\boldsymbol{x}^{(j.k)}$ are then extracted from $\boldsymbol{R}(\boldsymbol{x}^{(j.k)})$ which requires just one EM analysis of the antenna. In practice, a few EM analyses might be necessary in order to obtain more precise identification of the design that corresponds to a given perturbation of the objective vector (cf. (9)), which is arranged by embedding the solution process (9), (10) in a trust-region framework with the Jacobian $\boldsymbol{J}$ updated using the Broyden formula in each iteration [51]. The perturbations d_k are small (although their specific values are not critical). Therefore, we have

$$x_l^{(j.k)} \approx x_l^{(j)} + \sum_{r=1}^{N} J^x_{lr}(\boldsymbol{x}^{(j)})[f_r^{(j.k)} - f_r^{(j)}] \tag{11}$$

Equation (11) can be rewritten in the matrix form as follows

$$\boldsymbol{X} = \boldsymbol{J}^x \boldsymbol{F} \tag{12}$$

where

$$\boldsymbol{X} = \left[\boldsymbol{x}^{(j.1)} - \boldsymbol{x}^{(j)} \quad \cdots \quad \boldsymbol{x}^{(j.N)} - \boldsymbol{x}^{(j)}\right] \tag{13}$$

and

$$\boldsymbol{F} = \begin{bmatrix} f_1^{(j.1)} - f_1^{(j)} & \cdots & f_1^{(j.N)} - f_1^{(j.N)} \\ \vdots & \ddots & \vdots \\ f_N^{(j.1)} - f_N^{(j)} & \cdots & f_N^{(j.N)} - f_N^{(j.N)} \end{bmatrix} \tag{14}$$

If the matrix $\boldsymbol{F}$ is invertible, (12) can be solved analytically for $\boldsymbol{J}^x$ as

$$\boldsymbol{J}^x = \boldsymbol{X}\boldsymbol{F}^{-1} \tag{15}$$

For the special case when $[f_1^{(j.k)} \ldots f_N^{(j.k)}]^T = [f_1^{(j)} \ldots f_k^{(j)} + d_k \ldots f_N^{(j)}]^T$, the matrix $\boldsymbol{F}$ is diagonal, i.e., $\boldsymbol{F} = \text{diag}(d_1,\ldots, d_N)$. In practice, even though $[f_1^{(j.k)} \ldots f_N^{(j.k)}]^T \neq [f_1^{(j)} \ldots f_k^{(j)} + d_k \ldots f_N^{(j)}]^T$, off-diagonal elements are small, therefore non-singularity of $\boldsymbol{F}$ normally holds. Nevertheless, in the aforementioned special case, one has

$$x_l^{(j.k)} \approx x_l^{(j)} + J_{lk}^x(\boldsymbol{x}^{(j)})d_k \tag{16}$$

which implies

$$J_{lk}^x(\boldsymbol{x}^{(j)}) \approx \left[x_l^{(j.k)} - x_l^{(j)}\right]/d_k \tag{17}$$

Then, as $\boldsymbol{F} = \text{diag}(d_1,\ldots, d_N)$, (15) coincides with (17). Having $\{\boldsymbol{f}^{(j)}, \boldsymbol{x}^{(j)}, \boldsymbol{J}^x(\boldsymbol{f}^{(j)})\}, j = 1, \ldots, p$, the first-level model can be constructed using GEK, denoted as $\boldsymbol{s}_{1.GEK}(\boldsymbol{f})$. The benefit is a significantly smaller number of data samples required to yield the model as compared to the derivative-free version.

D. DOMAIN DEFINITION AND SECOND-LEVEL MODEL

As $\boldsymbol{s}_{1.GEK}(\boldsymbol{f})$ only approximates $X^*(F)$, the surrogate model domain X_S is defined by extending it to ensure that most of the designs $X^*(\boldsymbol{f}) \in X_S$. The extension is implemented using the vectors normal to $\boldsymbol{s}_{1.GEK}(F)$. An orthonormal basis of vectors normal to $\boldsymbol{s}_{1.GEK}(F)$ at $\boldsymbol{f}$ is denoted by $\{\boldsymbol{v}_n^{(k)}(\boldsymbol{f})\}, k = 1, \ldots, n - N$. These are used to define the extension coefficients

$$\begin{aligned}\boldsymbol{\alpha}(\boldsymbol{f}) &= [\alpha_1(\boldsymbol{f}) \ldots \alpha_{n-N}(\boldsymbol{f})]^T = \\ &= 0.5T\left[|\boldsymbol{x}_d \boldsymbol{v}_n^{(1)}(\boldsymbol{f})| \quad \ldots \quad |\boldsymbol{x}_d \boldsymbol{v}_n^{(n-N)}(\boldsymbol{f})|\right]^T\end{aligned} \tag{18}$$

where $\boldsymbol{x}_d = \boldsymbol{x}_{\max} - \boldsymbol{x}_{\min}$ (parameter variations within $\boldsymbol{s}_{1.GEK}(F)$) with $\boldsymbol{x}_{\max} = \max\{\boldsymbol{x}^{(k)}, k = 1, \ldots, p\}$ and $\boldsymbol{x}_{\min} = \min\{\boldsymbol{x}^{(k)}, k = 1, \ldots, p\}$; T is a user-defined thickness parameter (typically 0.05 to 0.1).

The domain X_S is allocated between the manifolds M_+ and M_-

$$M_\pm = \left\{\boldsymbol{x} \in X : \boldsymbol{x} = \boldsymbol{s}_{1.GEK}(\boldsymbol{f}) \pm \sum\nolimits_{k=1}^{n-N} \alpha_k(\boldsymbol{f})\boldsymbol{v}_n^{(k)}(\boldsymbol{f})\right\} \tag{19}$$

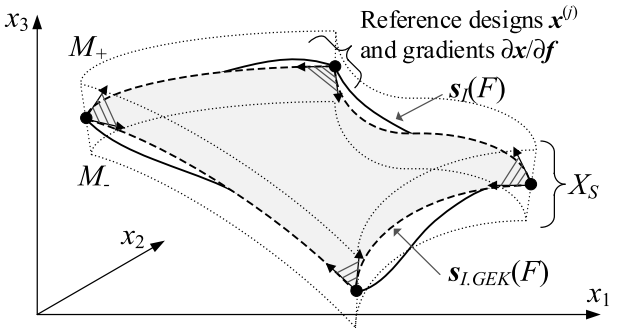

FIGURE 2. The image $\boldsymbol{s}_{1.GEK}(F)$ of the GEK-based first-level surrogate model, the manifolds M_- and M_+ and the surrogate model domain X_S defined as the orthogonal extension of $\boldsymbol{s}_{1.GEK}(F)$. Here, the first-level model is defined using the corner reference designs $\boldsymbol{x}^{(j)}$ only and their corresponding sensitivities $\partial\boldsymbol{x}/\partial\boldsymbol{f} = \partial\boldsymbol{X}^*(\boldsymbol{f}^{(j)})/\partial\boldsymbol{f}$ symbolically marked using arrows and gray shading.

therefore we have (see also Fig. 2)

$$X_S = \left\{\begin{array}{c}\boldsymbol{x} = \boldsymbol{s}_{1.GEK}(\boldsymbol{f}) + \sum\limits_{k=1}^{n-N} \lambda_k\alpha_k(\boldsymbol{f})\boldsymbol{v}_n^{(k)}(\boldsymbol{f}) : \boldsymbol{f} \in F, \\ -1 \le \lambda_k \le 1, \ k = 1, \ldots, n - N\end{array}\right\} \tag{20}$$

The final (second-level) surrogate is constructed similarly as in [48]. It is a kriging interpolation model identified within the domain X_S using the training data $\{\boldsymbol{x}_B^{(k)}, \boldsymbol{R}(\boldsymbol{x}_B^{(k)})\}_{k=1,\ldots,NB}$, where $\boldsymbol{x}_B^{(k)}$ are the samples uniformly allocated in X_S; recall that $\boldsymbol{R}$ stands for the response of the EM antenna model. Design of experiments and model optimization procedures have been explained in detail in [48]. The graphical illustration of the overall modeling procedure is shown in Fig. 3.

Confinement of the surrogate domain as described above permits construction of reliable surrogates using a reasonably small number of samples (typically, a few hundred [47], [48]). More importantly, this can be done without formally restricting the ranges of antenna parameters and its operating conditions. This is often beyond the reach of conventional modeling techniques, especially when the number of antenna parameters is large. As mentioned before, a typical number of reference designs varies from ten to twenty depending on the objective space dimensionality. Assuming that the computational cost of obtaining a reference design is several dozens of EM simulations, the overall related expenses may by far exceed the cost of training data acquisition within the domain X_S. As demonstrated in Section 3, constructing the first-level model using GEK allows for reduction of the number of reference designs along with the associated cost of their generation by at least fifty percent. This allows for a significant reduction of the overall computational cost of building a reliable surrogate model. At the same time, one needs to remember that a conventional, box-constrained domain, is also defined using the same reference designs (simply by taking the smallest box that contains all the reference designs). If these were not available, the box-constrained domain would have been much larger. Thus, the cost of finding the reference designs

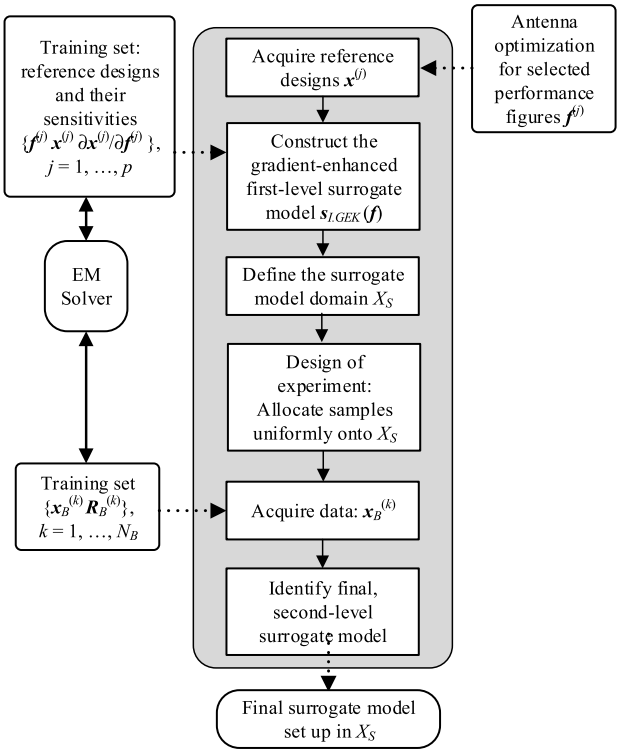

FIGURE 3. Flow diagram of the proposed gradient-enhanced kriging modeling bi-layer technique.

adds both to the constrained and the benchmark modeling methods.

III. NUMERICAL RESULTS

This section provides numerical verification of the proposed modelling methodology. The nested kriging framework with gradient-based first level model is compared to conventional nested kriging surrogate in terms of accuracy as well as computational cost. The following sections introduce the considered test cases, describe the experimental setup, and discuss the obtained results. Note that the reflection characteristic is selected as the antenna output to be modelled; however, the method is generic and allows modelling of any antenna responses. This is illustrated in the second example, where the realized gain is modelled along with the reflection response.

A. VERIFICATION CASE STUDIES

Numerical verification of the proposed approach is based on two antenna structures. The first one is a triple-band uniplanar dipole antenna shown in Fig. 4(a) (Antenna I) [52], implemented on RO4350 substrate ($\varepsilon_r = 3.48$, $h = 0.762$ mm) and fed by a coplanar waveguide. The geometry parameters of Antenna I are: $\boldsymbol{x} = [l_1\ l_2\ l_3\ l_4\ l_5\ w_1\ w_2\ w_3\ w_4\ w_5]^T$; whereas $l_0 = 30$, $w_0 = 3$, $s_0 = 0.15$ and $o = 5$ are fixed (all dimensions in mm). The full-wave electromagnetic model is implemented in CST Microwave Studio and simulated using its time-domain solver. The simulation time on dual Intel Xeon E5-2620 machine with 128 GB RAM is about 2 minutes.

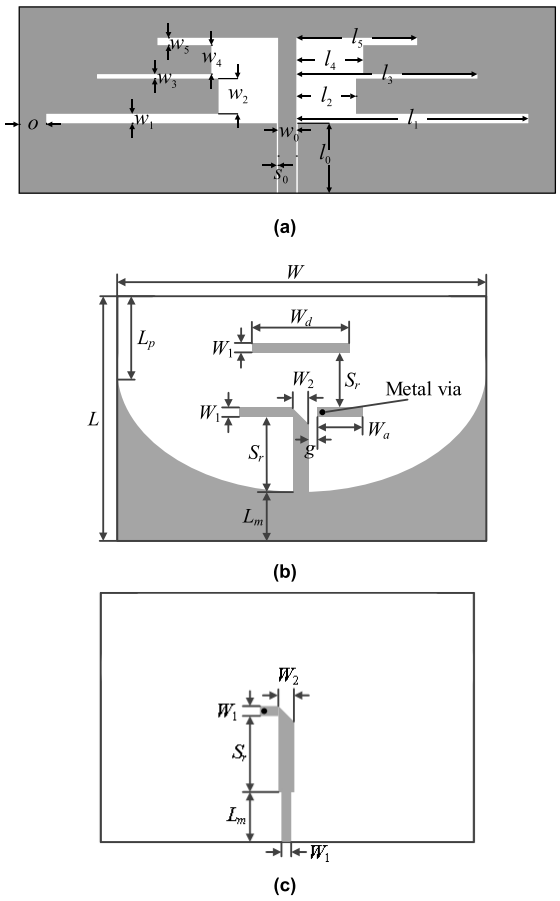

FIGURE 4. Verification case studies: (a) triple-band dipole antenna [52], quasi-Yagi antenna [53]: (b) top layer and (c) bottom layer.

The objective is to construct the surrogate valid for the operating frequencies f_k, $k = 1, 2, 3$, $f_2 = f_1k_1$, $f_3 = f_2k_2$, within the following ranges: 1.5 GHz $\leq f_1 \leq$ 2.5 GHz, $1.2 \leq k_1 \leq 1.6$, and $1.2 \leq k_2 \leq 1.6$. Thus, the objective space consists of the vectors $[f_1k_1\ k_2]^T$, and the operating frequencies f_2 and f_3 are computed according to the above formulas. Table 1 shows the data concerning reference designs considered for the conventional nested kriging framework of [48] as well as the approach proposed in this work. The lower and upper bounds for design variables are: $\boldsymbol{l} = [30\ 5.0\ 20\ 5.0\ 15\ 0.2\ 0.2\ 0.2\ 0.2\ 0.2]^T$, and $\boldsymbol{u} = [50\ 15\ 30\ 15\ 21\ 2.2\ 4.2\ 2.2\ 4.2\ 2.2]^T$ (both based on the reference design allocation).

The second verification case is a quasi-Yagi antenna of [53] (Antenna II), shown in Fig. 4(b). The geometry of the structure is described by the parameter vector $\boldsymbol{x} = [W\ L\ L_m\ L_p\ S_d S_r W_2 W_a W_d g]^T$ (all dimensions in mm). The antenna is implemented on 1.5-thick substrate, whereas the feed line width W_1 is calculated for a given substrate permittivity to ensure 50-ohm input impedance. The permittivity is used as one of the operating conditions, and, therefore, a part of the objective space for the modeling problem. Similarly as for Antenna I, the computational model is implemented in CST. The simulation time on dual Intel Xeon E5-2620 machine with 128 GB RAM is about 2.5 minutes.

TABLE 1. Reference design allocation for nested kriging and proposed gradient-based modelling technique.

Verification Case	Reference Designs			
	Conventional Nested Kriging [48]		Nested Kriging with Gradient-Based First-Level Model [This Work]	
	Design Allocation	Number of Reference Designs	Design Allocation	Number of Reference Designs
Antenna I	Designs corresponding to all combinations of $f_1 \in \{1.5, 2.0, 2.5\}$, $k_1 \in \{1.2, 1.4, 1.6\}$, $k_2 \in \{1.2, 1.4, 1.6\}$	**27**	Designs corresponding to objective space corners, i.e., $\{f_1,k_1,k_2\}$ = {1.5,1.2,1.2}, {1.5,1.2,1.6}, {1.5,1.6,1.2}, {1.5,1.6,1.6}, {2.5,1.2,1.2}, {2.5,1.2,1.6}, {2.5,1.6,1.2}, {2.5,1.6,1.6},	**8**
Antenna II	Designs corresponding to pairs $\{f_0,\varepsilon_r\}$ = {2.5, 4.5}, {3.5, 4.5}, {5.0, 4.5}, {2.5, 2.5}, {5.0, 2.5}, {3.5, 2.5}, {4.5, 3.5}, {3.0, 3.5}	**8**	Designs corresponding to objective space corners, i.e., $\{f_0,\varepsilon_r\}$ = {2.5, 4.5}, {5.0, 4.5}, {2.5, 2.5}, {5.0, 2.5}	**4**

TABLE 2. Modeling results and benchmarking for Antenna I.

Number of Training Samples	Relative RMS Error			
	Conventional Kriging Model	Conventional RBF	Conventional Nested Kriging Model [48]	GEK-based Nested Kriging Model [this work]
50	22.7 %	23.5 %	16.0 %	18.6 %
100	19.9 %	19.8 %	11.2 %	13.5 %
200	18.6 %	19.2 %	9.9 %	10.1 %
400	17.2 %	18.8 %	9.7 %	8.9 %
800	16.8 %	17.4 %	7.8 %	7.1 %

The goal is to render the surrogate valid over the antenna operating frequency f_0 from 2.5 GHz to 5.0 GHz, and the substrate permittivity ε_r from 2.5 to 4.5. Here, the responses of interest are reflection and realized gain characteristics. The design optimality conditions for a given substrate permittivity ε_r are the following: (i) given the center frequency f_0, ensure at least 8-percent fractional bandwidth (symmetric w.r.t. f_0), (ii) maximize the average realized gain within the same 8-percent bandwidth. The data on the reference design allocation for the conventional nested kriging framework and proposed technique can be found in Table 1. The conventional space X is defined by the lower bounds $\boldsymbol{l} = [100\ 55\ 10\ 14.5\ 6.0\ 10\ 2.0\ 7.5\ 16.3\ 0.5]^T$, and upper bounds $\boldsymbol{u} = [137\ 81\ 29\ 28\ 21\ 18\ 5.0\ 20\ 40\ 1.0]^T$.

B. EXPERIMENTAL SETUP

The proposed surrogate model has been constructed for both considered antennas and for various training data set sizes: 50, 100, 200, 400, and 800 samples. The assumed error measure is relative a RMS error averaged over the independent set of 100 testing samples. For comparison, the proposed technique has been compared to conventional nested kriging using non-sensitivity based first-level model (cf. Table 1 for the data on reference designs). In both cases, the models are obtained for the thickness parameter $T = 0.05$. As mentioned before, the primary advantage of gradient-based first level model is a significantly smaller number of reference designs (by a factor of three and two for Antenna I and II, respectively).

Our objective is to verify whether incorporating gradient-based first-level model does not have a detrimental effect on the predictive power of the surrogate models. For completeness, both versions of the nested kriging approach are compared to conventional models (kriging and radial basis function surrogates).

TABLE 3. Modeling results and benchmarking for Antenna II.

Number of Training Samples	Relative RMS Error			
	Conventional Kriging Model	Conventional RBF	Conventional Nested Kriging Model [48]	GEK-based Nested Kriging Model [this work]
50	61.4 %	65.3 %	17.9 %	10.6 %
100	50.7 %	51.8 %	13.3 %	7.3 %
200	39.8 %	43.2 %	7.5 %	6.5 %
400	32.8 %	37.1 %	5.4 %	6.0 %
800	31.8 %	33.6 %	4.5 %	5.1 %

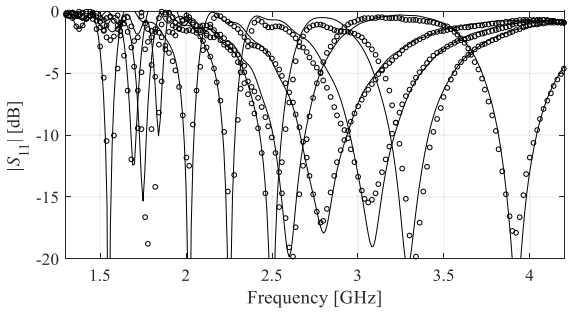

FIGURE 5. Reflection characteristics of the antenna of Fig. 4(a) at the selected test designs: EM simulation model (—), and the proposed surrogate (o). The surrogate set up using N= 400 training samples.

C. RESULTS AND DISCUSSION

The numerical results obtained for Antennas I and II are shown in Tables 2 and 3, as well as in Figs. 5 and 6. Both versions of the nested kriging surrogates are significantly better than conventional models (see, e.g., [48] for details). However, the main point of this section is to demonstrate that a significant reduction of the number of reference designs (thus, a reduction of the overall cost of the model process) offered by the GEK-based approach is achieved without compromising the modeling accuracy. The data in Tables 2 and 3 indicates that this is indeed the case. The accuracy of the conventional and the proposed nested surrogates are very much comparable for both considered antenna structures and for all training data sets. The differences are minor and statistically insignificant.

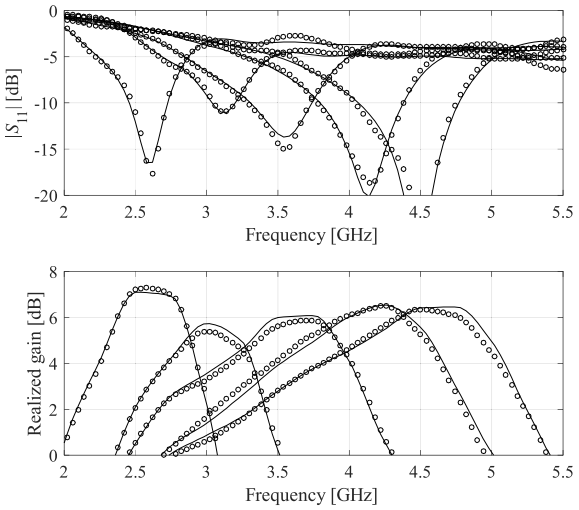

FIGURE 6. Characteristics of the antenna of Fig. 4(b) at the selected test designs: EM simulation model (—), and the proposed surrogate (o). The surrogate set up using $N = 400$ training samples. The top and bottom plots illustrate the reflection and realized gain characteristics, respectively.

IV. CONCLUSION

The paper proposed a novel technique for surrogate modelling of antenna structures. Our methodology combines the recently introduced nested kriging framework and gradient-based kriging utilized to construct the first-level surrogate of the nester kriging. As a part of this endeavour, a rigorous and cost-efficient procedure for estimating the gradients of antenna geometry parameters with respect to the figures of interest pertinent to the modelling process has been developed as well. The major computational benefit of the presented approach is a significant reduction of the number of reference designs necessary to render the first-level model (the latter required to define the surrogate model domain), by a factor of two, or even three for the objective spaces of higher dimensions. This directly translates into a reduced initial cost of the modelling process as all reference designs need to be pre-optimized beforehand. The proposed technique has been comprehensively validated using two antenna structures described by ten parameters each, with the surrogates covering broad ranges of antenna dimensions and operating conditions. The obtained results demonstrate that reducing the number of reference designs does not have a negative effect on the model predictive power. Consequently, by addressing one of the practical issues of nested kriging, our method can be considered a major step forward in the development of performance-driven modelling frameworks.

ACKNOWLEDGMENT

The authors would like to thank Dassault Systemes, France, for making CST Microwave Studio available.

REFERENCES

[1] X. Cheng, Y. Yao, T. Yu, Z. Chen, J. Yu, and X. Chen, "Analysis and design of a low-cost circularly polarized horn antenna," *IEEE Trans. Antennas Propag.*, vol. 66, no. 12, pp. 7363–7367, Dec. 2018.
[2] M.-N. Chen, W.-J. Lu, L.-J. Wang, M. Yang, and L. Zhu, "Design approach to a novel planar bisensing circularly polarized antenna," *IEEE Trans. Antennas Propag.*, vol. 67, no. 11, pp. 6839–6846, Nov. 2019.
[3] C. Borda-Fortuny, L. Cai, K. F. Tong, and K.-K. Wong, "Low-cost 3D-printed coupling-fed frequency agile fluidic monopole antenna system," *IEEE Access*, vol. 7, pp. 95058–95064, 2019.
[4] B. Gong, Q. R. Zheng, X. S. Ren, Y. Y. Zeng, and L. H. Su, "Compact slot antenna for ultra-wide band applications," *IET Microw., Antennas Propag.*, vol. 8, no. 3, pp. 200–205, Feb. 2014.
[5] P. S. M. Yazeen, C. V. Vinisha, S. Vandana, M. Suprava, and R. U. Nair, "Electromagnetic performance analysis of graded dielectric inhomogeneous streamlined airborne radome," *IEEE Trans. Antennas Propag.*, vol. 65, no. 5, pp. 2718–2723, May 2017.
[6] S. Kim and S. Nam, "A compact and wideband linear array antenna with low mutual coupling," *IEEE Trans. Antennas Propag.*, vol. 67, no. 8, pp. 5695–5699, Aug. 2019.
[7] L. Y. Nie, X. Q. Lin, Z. Q. Yang, J. Zhang, and B. Wang, "Structure-shared planar UWB MIMO antenna with high isolation for mobile platform," *IEEE Trans. Antennas Propag.*, vol. 67, no. 4, pp. 2735–2738, Apr. 2019.
[8] J. Zeng and K.-M. Luk, "Single-layered broadband magnetoelectric dipole antenna for new 5G application," *IEEE Antennas Wireless Propag. Lett.*, vol. 18, no. 5, pp. 911–915, May 2019.
[9] J. M. Felicio, J. M. Bioucas-Dias, J. R. Costa, and C. A. Fernandes, "Antenna design and near-field characterization for medical microwave imaging applications," *IEEE Trans. Antennas Propag.*, vol. 67, no. 7, pp. 4811–4824, Jul. 2019.
[10] K. R. Jha, B. Bukhari, C. Singh, G. Mishra, and S. K. Sharma, "Compact planar multistandard MIMO antenna for IoT applications," *IEEE Trans. Antennas Propag.*, vol. 66, no. 7, pp. 3327–3336, Jul. 2018.
[11] J.-F. Qian, F.-C. Chen, K.-R. Xiang, and Q.-X. Chu, "Resonator-loaded multi-band microstrip slot antennas with bidirectional radiation patterns," *IEEE Trans. Antennas Propag.*, vol. 67, no. 10, pp. 6661–6666, Oct. 2019.
[12] U. Ullah and S. Koziel, "A broadband circularly polarized wide-slot antenna with a miniaturized footprint," *IEEE Antennas Wireless Propag. Lett.*, vol. 17, no. 12, pp. 2454–2458, Dec. 2018.
[13] Y. Dong, J. Choi, and T. Itoh, "Vivaldi antenna with pattern diversity for 0.7 to 2.7 GHz cellular band applications," *IEEE Antennas Wireless Propag. Lett.*, vol. 17, no. 2, pp. 247–250, Feb. 2018.
[14] S. Yan, P. J. Soh, and G. A. E. Vandenbosch, "Wearable dual-band magneto-electric dipole antenna for WBAN/WLAN applications," *IEEE Trans. Antennas Propag.*, vol. 63, no. 9, pp. 4165–4169, Sep. 2015.
[15] J. Wang, M. Leach, E. G. Lim, Z. Wang, R. Pei, and Y. Huang, "An implantable and conformal antenna for wireless capsule endoscopy," *IEEE Antennas Wireless Propag. Lett.*, vol. 17, no. 7, pp. 1153–1157, Jul. 2018.
[16] M. A. Fakih, A. Diallo, P. Le Thuc, R. Staraj, O. Mourad, and E. A. Rachid, "Optimization of efficient dual band PIFA system for MIMO half-duplex 4G/LTE and full-duplex 5G communications," *IEEE Access*, vol. 7, pp. 128881–128895, 2019.
[17] K. Tsukamoto and H. Arai, "Optimization of smooth walled horn antenna using multilevel fast multipole method," in *Proc. Int. Symp. Ant. Prop. (ISAP)*, Okinawa, Japan, Oct. 2016, pp. 416–417.
[18] A. Lalbakhsh, M. U. Afzal, and K. P. Esselle, "Multiobjective particle swarm optimization to design a time-delay equalizer metasurface for an electromagnetic band-gap resonator antenna," *IEEE Antennas Wireless Propag. Lett.*, vol. 16, pp. 912–915, 2017.
[19] S. Koziel and S. Ogurtsov, *Simulation-Based Optimization Of Antenna Arrays*. Singapore: World Scientific, 2019.
[20] S. Koziel, Q. S. Cheng, J. W. Bandler, and S. Ogurtsov, "Rapid electromagnetic-based microwave design optimisation exploiting shape-preserving response prediction and adjoint sensitivities," *IET Microw., Antennas Propag.*, vol. 8, no. 10, pp. 775–781, Jul. 2014.
[21] S. Koziel and A. Pietrenko-Dabrowska, "Reduced-cost electromagnetic-driven optimisation of antenna structures by means of trust-region gradient-search with sparse Jacobian updates," *IET Microw., Antennas Propag.*, vol. 13, no. 10, pp. 1646–1652, Aug. 2019.
[22] S. Koziel and A. Pietrenko-Dabrowska, "Variable-fidelity simulation models and sparse gradient updates for cost-efficient optimization of compact antenna input characteristics," *Sensors*, vol. 19, no. 8, p. 1806, Apr. 2019.
[23] S. Koziel, Q. S. Cheng, and J. W. Bandler, "Space mapping," *IEEE Microw. Mag.*, vol. 9, no. 6, pp. 105–122, Dec. 2008.
[24] S. Koziel and S. Ogurtsov, "Rapid design of microstrip antenna arrays by means of surrogate-based optimisation," *IET Microw., Antennas Propag.*, vol. 9, no. 5, pp. 463–471, Apr. 2015.

[25] J. E. Rayas-Sanchez, "Power in simplicity with ASM: Tracing the aggressive space mapping algorithm over two decades of development and engineering applications," *IEEE Microw. Mag.*, vol. 17, no. 4, pp. 64–76, Apr. 2016.
[26] Y. Su, J. Li, Z. Fan, and R. Chen, "Shaping optimization of double reflector antenna based on manifold mapping," in *Proc. Int. Applied Comput. Electromagn. Soc. Symp. (ACES)*, Suzhou, China, Aug. 2017, pp. 1–2.
[27] S. Koziel and S. D. Unnsteinsson, "Expedited design closure of antennas by means of trust-region-based adaptive response scaling," *IEEE Antennas Wireless Propag. Lett.*, vol. 17, no. 6, pp. 1099–1103, Jun. 2018.
[28] S. Koziel, "Fast simulation-driven antenna design using response-feature surrogates," *Int. J. RF Microw. Comput.-Aided Eng.*, vol. 25, no. 5, pp. 394–402, Jun. 2015.
[29] C. Zhang, F. Feng, V.-M.-R. Gongal-Reddy, Q. J. Zhang, and J. W. Bandler, "Cognition-driven formulation of space mapping for equal-ripple optimization of microwave filters," *IEEE Trans. Microw. Theory Techn.*, vol. 63, no. 7, pp. 2154–2165, Jul. 2015.
[30] J. A. Easum, J. Nagar, and D. H. Werner, "Multi-objective surrogate-assisted optimization applied to patch antenna design," in *Proc. Int. Symp. Antennas Propag. (ISAP)*, San Diego, CA, USA, 2017, pp. 339–340.
[31] D. I. L. de Villiers, I. Couckuyt, and T. Dhaene, "Multi-objective optimization of reflector antennas using kriging and probability of improvement," in *Proc. Int. Symp. Antennas Propag. (ISAP)*, San Diego, CA, USA, 2017, pp. 985–986.
[32] J. Dong, W. Qin, and M. Wang, "Fast multi-objective optimization of multi-parameter antenna structures based on improved BPNN surrogate model," *IEEE Access*, vol. 7, pp. 77692–77701, 2019.
[33] J. Tak, A. Kantemur, Y. Sharma, and H. Xin, "A 3-D-printed W-band slotted waveguide array antenna optimized using machine learning," *IEEE Antennas Wireless Propag. Lett.*, vol. 17, no. 11, pp. 2008–2012, Nov. 2018.
[34] H. M. Torun and M. Swaminathan, "High-dimensional global optimization method for high-frequency electronic design," *IEEE Trans. Microw. Theory Techn.*, vol. 67, no. 6, pp. 2128–2142, Jun. 2019.
[35] N. V. Queipo, R. T. Haftka, W. Shyy, T. Goel, R. Vaidynathan, and P. K. Tucker, "Surrogate based analysis and optimization," *Prog. Aerosp. Sci.*, vol. 41, no. 1, pp. 1–28, 2005.
[36] P. Barmuta, F. Ferranti, G. P. Gibiino, A. Lewandowski, and D. M. M.-P. Schreurs, "Compact behavioral models of nonlinear active devices using response surface methodology," *IEEE Trans. Microw. Theory Techn.*, vol. 63, no. 1, pp. 56–64, Jan. 2015.
[37] J. Cai, J. King, C. Yu, J. Liu, and L. Sun, "Support vector regression-based behavioral modeling technique for RF power transistors," *IEEE Microw. Wireless Compon. Lett.*, vol. 28, no. 5, pp. 428–430, May 2018.
[38] J. P. Jacobs, "Characterisation by Gaussian processes of finite substrate size effects on gain patterns of microstrip antennas," *IET Microw., Antennas Propag.*, vol. 10, no. 11, pp. 1189–1195, Aug. 2016.
[39] J. Du and C. Roblin, "Stochastic surrogate models of deformable antennas based on vector spherical harmonics and polynomial chaos expansions: Application to textile antennas," *IEEE Trans. Antennas Propag.*, vol. 66, no. 7, pp. 3610–3622, Jul. 2018.
[40] C. Cai, S. Bilicz, T. Rodet, M. Lambert, and D. Lesselier, "Metamodel-based nested sampling for model selection in eddy-current testing," *IEEE Trans. Magn.*, vol. 53, no. 4, Apr. 2017, Art. no. 6200912.
[41] A. C. Yücel, H. Bagci, and E. Michielssen, "An ME-PC enhanced HDMR method for efficient statistical analysis of multiconductor transmission line networks," *IEEE Trans. Compon., Packag., Manuf. Technol.*, vol. 5, no. 5, pp. 685–696, May 2015.
[42] R. Hu, V. Monebhurrun, R. Himeno, H. Yokota, and F. Costen, "An adaptive least angle regression method for uncertainty quantification in FDTD computation," *IEEE Trans. Antennas Propag.*, vol. 66, no. 12, pp. 7188–7197, Dec. 2018.
[43] M. C. Kennedy and A. O'Hagan, "Predicting the output from a complex computer code when fast approximations are available," *Biometrika*, vol. 87, no. 1, pp. 1–13, Mar. 2000.
[44] J. P. Jacobs and S. Koziel, "Two-stage framework for efficient Gaussian process modeling of antenna input characteristics," *IEEE Trans. Antennas Propag.*, vol. 62, no. 2, pp. 706–713, Feb. 2014.
[45] F. Wang, P. Cachecho, W. Zhang, S. Sun, X. Li, R. Kanj, and C. Gu, "Bayesian model fusion: Large-scale performance modeling of analog and mixed-signal circuits by reusing early-stage data," *IEEE Trans. Comput.-Aided Design Integr. Circuits Syst.*, vol. 35, no. 8, pp. 1255–1268, Aug. 2016.
[46] S. Koziel, "Low-cost data-driven surrogate modeling of antenna structures by constrained sampling," *IEEE Antennas Wireless Propag. Lett.*, vol. 16, pp. 461–464, 2017.
[47] S. Koziel and A. T. Sigurdsson, "Triangulation-based constrained surrogate modeling of antennas," *IEEE Trans. Antennas Propag.*, vol. 66, no. 8, pp. 4170–4179, Aug. 2018.
[48] S. Koziel and A. Pietrenko-Dabrowska, "Performance-based nested surrogate modeling of antenna input characteristics," *IEEE Trans. Antennas Propag.*, vol. 67, no. 5, pp. 2904–2912, May 2019.
[49] A. I. J. Forrester and A. J. Keane, "Recent advances in surrogate-based optimization," *Prog. Aerosp. Sci.*, vol. 45, nos. 1–3, pp. 50–79, Jan. 2009.
[50] M. D. Morris, T. J. Mitchell, and D. Ylvisaker, "Bayesian design and analysis of computer experiments: Use of derivatives in surface prediction," *Technometrics*, vol. 35, no. 3, pp. 243–255, Aug. 1993.
[51] J. Nocedal and S. Wright, *Numerical Optimization*, 2nd ed. New York, NY, USA: Springer, 2006.
[52] Y.-C. Chen, S.-Y. Chen, and P. Hsu, "Dual-band slot dipole antenna fed by a coplanar waveguide," in *Proc. IEEE Int. Symp. Antennas Propag. (ISAP)*, Jul. 2006, pp. 3589–3592.
[53] Z. Hua, G. Haichuan, L. Hongmei, L. Beijia, L. Guanjun, and W. Qun, "A novel high-gain quasi-Yagi antenna with a parabolic reflector," in *Proc. Int. Symp. Antennas Propag. (ISAP)*, Hobart, TAS, Australia, Nov. 2015, pp. 1–3.

ANNA PIETRENKO-DABROWSKA (Senior Member, IEEE) received the M.Sc. and Ph.D. degrees in electronic engineering from the Gdansk University of Technology, Poland, in 1998 and 2007, respectively. She is currently an Associate Professor with the Gdansk University of Technology. Her research interests include simulation-driven design, design optimization, control theory, modeling of microwave and antenna structures, and numerical analysis.

SLAWOMIR KOZIEL (Senior Member, IEEE) received the M.Sc. and Ph.D. degrees in electronic engineering from the Gdansk University of Technology, Poland, in 1995 and 2000, respectively, and the M.Sc. degrees in theoretical physics and mathematics and the Ph.D. degree in mathematics from the University of Gdansk, Poland, in 2000, 2002, and 2003, respectively. He is currently a Professor with the Department of Engineering, Reykjavik University, Iceland. His research interests include CAD and modeling of microwave and antenna structures, simulation-driven design, surrogate-based optimization, space mapping, circuit theory, analog signal processing, evolutionary computation, and numerical analysis.

MU'ATH AL-HASAN (Senior Member, IEEE) received the B.Sc. degree in electrical engineering from the Jordan University of Science and Technology, Jordan, in 2005, the M.Sc. degree in wireless communications from Yarmouk University, Jordan, in 2008, and the Ph.D. degree in telecommunication engineering from the Institut National de la Recherche Scientifique (INRS), Université du Québec, Canada, in 2015. From 2013 to 2014, he was with Planets Inc., San Francisco, CA, USA. In May 2015, he joined Concordia University, Canada, as a Postdoctoral Fellowship. He is currently an Assistant Professor with Al Ain University, United Arab Emirates. His current research interests include antenna design at millimeter-wave and terahertz, channel measurements in multiple-input and multiple-output (MIMO) systems, machine learning, and artificial intelligence in antenna design.